Analysis of PANoptosis-related genes in septic cardiomyopathy by bioinformatics, machine learning and experimental validation

YIHENG YANG[1*], JIAHAO ZOU[1*], PENG YANG[1], ZHENZHONG ZHENG[1,2] and QINGSHAN TIAN[1]

[1]Department of Cardiology, The First Affiliated Hospital, Jiangxi Medical College, Nanchang University, Nanchang, Jiangxi 330006, P.R. China; [2]Department of Cardiology, Shenzhen Third People's Hospital, Shenzhen, Guangdong 518112, P.R. China

Received July 3, 2025; Accepted October 30, 2025

DOI: 10.3892/etm.2025.13050

Abstract. The mechanisms underlying the pathogenesis of septic cardiomyopathy (SCM) are intricate and incompletely understood. PANoptosis is a novel type of programmed cell death, and in the present study, bioinformatics, machine learning and experimental validation were used to identify key PANoptosis-related genes (PRGs) associated with SCM. Differentially expressed genes were obtained through analysis of the Gene Expression Omnibus dataset, and these genes were intersected with the PRGs to obtain the differentially expressed PRGs. Three machine learning algorithms were used to screen key PRGs; CIBERSORT was used for immune infiltration analysis and the diagnostic value of key PRGs was evaluated by plotting receiver operating characteristic curves. Additionally, a competitive endogenous (ce) RNA regulatory network analysis was conducted, and drug prediction analysis was performed. Finally, the expression of key PRGs was verified via quantitative PCR. A total of 157 differentially expressed genes and 21 differentially expressed PRGs were screened. In addition, two key PRGs (RIPK2 and GADD45B) were screened using least absolute shrinkage and selection operator regression, the support vector machine-recursive feature elimination algorithm and the random forest algorithm, with both genes demonstrating a high diagnostic value. RIPK2 and GADD45B were positively correlated with neutrophils. The ceRNA regulatory network included two mRNAs, eight microRNAs and 16 long noncoding RNAs and 10 drugs/molecular compounds were predicted. Finally, quantitative PCR results revealed that the expression of both RIPK2 and GADD45B was upregulated in the lipopolysaccharide-induced HL-1 cell injury model. In conclusion, the present study identified two key PRGs (RIPK2 and GADD45B) associated with SCM; these findings may lead to the development of novel diagnostic and therapeutic approaches for SCM.

Correspondence to: Professor Qingshan Tian or Professor Zhenzhong Zheng, Department of Cardiology, The First Affiliated Hospital, Jiangxi Medical College, Nanchang University, 17 Yongwaizheng Street, Nanchang, Jiangxi 330006, P.R. China
E-mail: ndyfy10093@ncu.edu.cn
E-mail: greateful@163.com

*Contributed equally

Key words: PANoptosis, sepsis, septic cardiomyopathy, machine learning, bioinformatics

Introduction

Sepsis is a systemic inflammatory syndrome caused by pathogens invading an organism, often resulting in organ dysfunction (1). It has been reported that the annual global incidence of sepsis ranges from 276-678 cases/100,000 population (2). Severe cases of sepsis can present as septic cardiomyopathy (SCM), which is defined as sepsis combined with cardiac dysfunction (3). Due to the lack of uniform diagnostic criteria, the reported incidence rates of SCM vary widely (4); however, a recent meta-analysis estimated the incidence of SCM in sepsis patients at ~20% (5). Patients with sepsis-induced cardiovascular disease usually have a poor prognosis, and according to previous studies, the mortality rate of patients with SCM can be as high as 70% (6), presenting a notable challenge for the healthcare community. The current low diagnostic rate and poor therapeutic efficacy of SCM highlight the need to improve diagnostic efficiency and explore novel therapeutic options.

The pathogenesis of sepsis has been partially explored and is considered to mainly involve the inflammatory response, mitochondrial damage, altered nitric oxide metabolism, apoptosis, ferroptosis and autonomic dysregulation (7-10). However, effective treatments for sepsis are still lacking; therefore, exploring the pathogenesis of SCM and developing targeted therapies would markedly improve the prognosis of patients with sepsis. Programmed cell death includes apoptosis, pyroptosis and necroptosis; in addition, Malireddi *et al* (11) proposed a novel type of programmed cell death called PANoptosis, which is mainly regulated by the PANoptosome complex. PANoptosis is characterized by three simultaneous types of cell death, including apoptosis, pyroptosis and necroptosis, and cannot be replaced with any single type of cell death (12). PANoptosis is associated with numerous conditions such as infectious and autoimmune diseases (13), and in sepsis-induced respiratory disease, it has been shown that PANoptosis is involved in sepsis-induced lung injury (14). In sepsis-induced neurological

disorders, the inhibition of PANoptosis via the downregulation of toll-like receptor 9 leads to improved survival in rats with sepsis-associated encephalopathy (15). These studies suggest a strong association between sepsis-related complications and PANoptosis. However, there are few studies on PANoptosis and sepsis-induced myocardial injury.

In the present study, gene expression profiles of the appropriate samples from the Gene Expression Omnibus (GEO) database were analyzed. The differentially expressed PANoptosis-related genes (PRGs) between the SCM group and the control group were subsequently identified. Additionally, three machine learning algorithms were employed to identify key genes, and experimental validation was performed. This study aimed to provide new insights into the diagnosis and treatment of SCM.

Materials and methods

Data sources. Gene expression datasets (GSE79962, GSE53007 and GSE142615) (16-18) were downloaded from the GEO database (http://www.ncbi.nlm.nih.gov/geo/). The GSE79962 dataset (GPL6244 platform) contains 31 available myocardial tissue samples (20 patients with SCM and 11 healthy controls). The GSE142615 dataset (GPL27951 platform) contains eight available myocardial tissue samples [four lipopolysaccharide (LPS)-induced myocardial injury mice and four healthy mice]. The GSE53007 dataset (GPL6885 platform) also contains eight available heart tissue samples (four SCM mice and four healthy mice).

Identification of differentially expressed genes (DEGs) and differentially expressed PRGs. Datasets were screened for DEGs using the 'limma' R package (version 3.56.2) (19). DEGs were defined as genes with adjusted $P<0.05$ and a fold change (FC) of $|\log2FC|>1$. For visual presentation of the results, volcano maps and heatmaps were plotted using the ggplot2 package (version 3.5.1) (20) and pheatmap package (version 1.0.12) (21) of R, respectively. A total of 902 PRGs were derived from published literature (22); subsequently, the PRGs were intersected with DEGs to obtain differentially expressed PRGs. Venn diagrams were created using an online tool (https://bioinformatics.psb.ugent.be/webtools/Venn/).

Functional enrichment analysis. Gene Ontology (GO) (23) and Kyoto Encyclopedia of Genes and Genomes (KEGG) (24) enrichment analyses of the differentially expressed PRGs were performed using the 'clusterProfiler' R package (25). GO analysis aimed to identify the cellular component (CC), molecular function (MF) and biological process (BP) terms enriched by the differentially expressed PRGs. The KEGG analysis sought to determine the pathways in which the differentially expressed PRGs were enriched. The results of the enrichment analyses are presented in columns and bubble charts.

Identification of key genes by machine learning and receiver operating characteristic (ROC) curve analysis. Least absolute shrinkage and selection operator (LASSO) regression, support vector machine-recursive feature elimination (SVM-RFE) and random forest (RF) methods are often used in bioinformatics to screen characteristic genes (26,27). These three machine learning algorithms were used to screen key genes in the differentially expressed PRGs. The advantage of LASSO is that it can automatically perform feature selection by reducing the coefficients of unimportant features to zero. This method eliminates most of the irrelevant or low-impact genes, leaving only a few genes with nonzero coefficients. The 'glmnet' R package (version 4.1-8) (28) was used to perform the LASSO regression analysis, and the α parameter was set to 1 and a 10-fold cross-validation scheme was used. The SVM-RFE algorithm is a commonly used feature selection method that combines the advantages of SVM and RFE. SVM is mainly used for solving classification problems and enables the separation of samples from different classes, and the RFE algorithm removes unimportant features in each iteration. The SVM-RFE analysis was performed using the 'e1071' (version 1.7-14) (29), 'caret' (version 6.0-94) (30) and 'kernlab' (version 0.9-32) (31) R packages; a 10-fold cross-validation scheme was used. The RF is used to build a more robust model by combining multiple simple decision trees; this algorithm can markedly reduce the risk of overfitting. The 'randomForest' package (version 4.7-1.1) (32) was used for RF analysis, with the ntree parameter set to 500, and genes with MeanDecreaseGini >2 were screened. The key genes were obtained via intersection analysis on the basis of the results of LASSO regression, SVM-RFE and RF. ROC curves were generated via the 'pROC' R package (version 1.18.5) (33) to analyze the diagnostic value of key genes for SCM.

Immune infiltration analysis. CIBERSORT (https://cibersortx.stanford.edu/) was used for immune infiltration analysis; it is a widely used computational method (34,35) for immunological studies that enables analysis of the proportions of different immune cell subpopulations in tissues using gene expression data. The matrix data of the related samples in the GSE79962 dataset were uploaded to CIBERSORTx, with LM22 used as the feature matrix (36). The results from the website provided the proportions of 22 immune cell types in each sample, with the results presented in a bar chart. The associations between the expression of key PRGs and 22 immune cell types were explored using Spearman's correlation analysis, with the results presented in lollipop charts.

Validation of key genes in the external dataset. For the validation set, the GSE53007 and GSE142615 datasets were combined. The expression of key PRGs was studied in the validation set, and the Wilcoxon rank-sum test was used to determine whether the key genes were differentially expressed between the SCM group and the control group. $P<0.05$ was considered to indicate a statistically significant difference. The results are presented in box plots.

Single-gene gene set enrichment analysis (GSEA). To investigate the effects of the expression of key genes on pathways, single-gene GSEA was performed. Patients with sepsis in the GSE79962 dataset were categorized into high- and low-expression groups based on the median expression level of the key PRGs. By comparing the transcriptomic profiles between the high- and low-expression groups and performing enrichment analysis, signaling pathways that are associated with changes in the expression of the key gene were identified; this approach

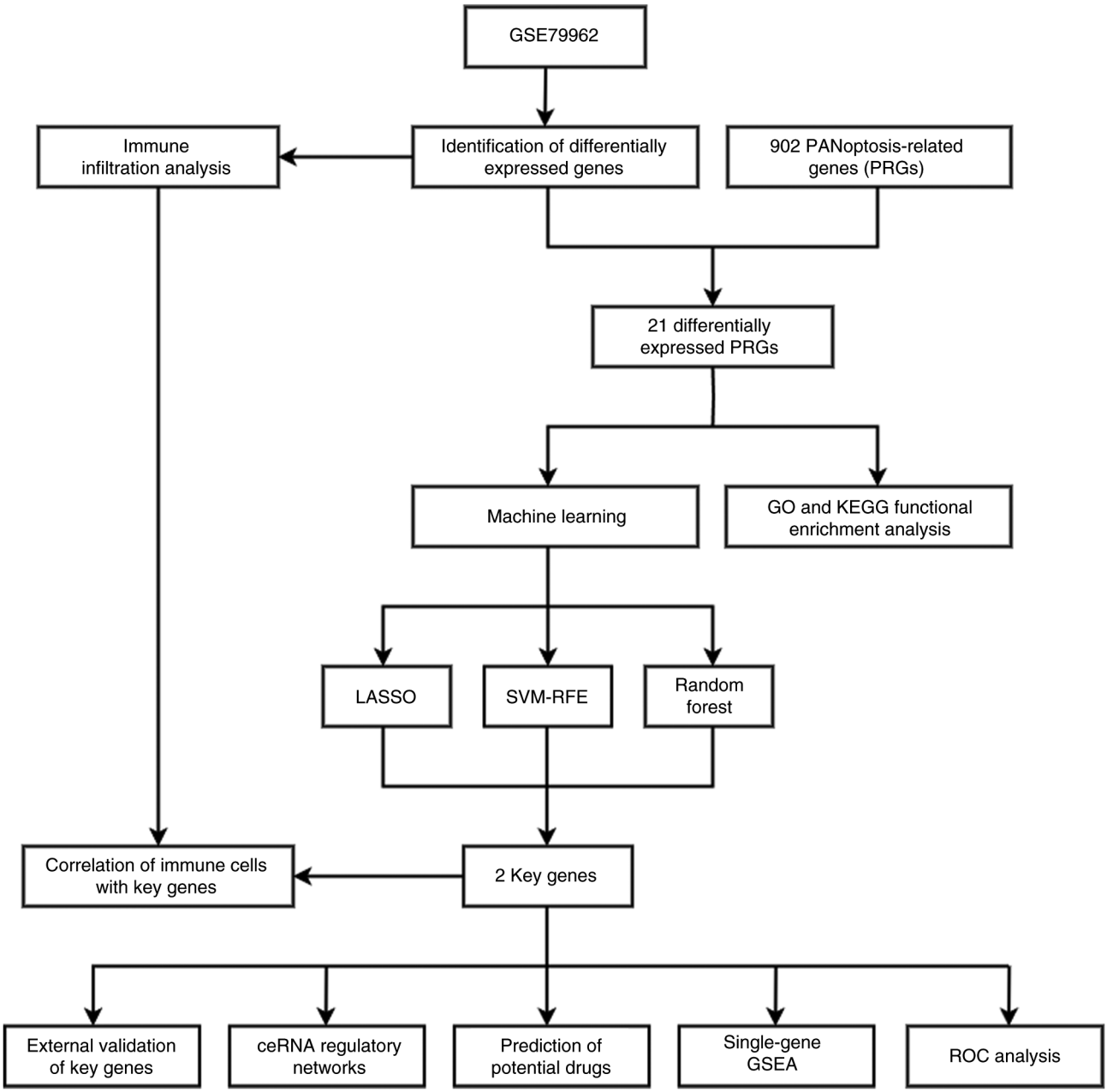

Figure 1. Flow chart of the present study. PRGs, PANoptosis-related genes; GO, Gene Ontology; KEGG, Kyoto Encyclopedia of Genes and Genomes; LASSO, least absolute shrinkage and selection operator; SVM-RFE, support vector machine-recursive feature elimination; ceRNA, competitive endogenous RNA; GSEA, gene set enrichment analysis; ROC, receiver operating characteristic.

has been applied in multiple previous studies (37-39). The criterion for significant enrichment was defined as $q<0.05$, adjusted $P<0.05$ and |normalized enrichment score|>1. Single-gene GSEA was performed using the 'clusterProfiler' R package (25), with part of the results presented.

Construction of competitive endogenous RNA (ceRNA) regulatory networks. A ceRNA regulatory network was constructed based on the key genes. The miRanda (40), miRDB (41), miRWalk (42) and TargetScan (43) databases were used to predict microRNAs (miRNAs). The miRNAs that appeared simultaneously in the aforementioned databases were used to construct the ceRNA regulatory network. The miRNAs were matched using the spongeScan (44) database to identify the corresponding long noncoding RNAs (lncRNAs). Cytoscape (version 3.9.1; https://cytoscape.org/) was used to visualize the ceRNA regulatory network.

Prediction of potential drugs. Currently, there are limited therapeutic drugs available for the treatment of SCM; therefore, the drugs associated with key PRGs were accessed through the Drug-Gene Interaction Database (DGIDB; https://dgidb.org/). The results were visualized using Cytoscape (version 3.9.1).

Cell culture and treatment. HL-1 cells (Procell Life Science & Technology Co., Ltd.) were cultured in minimum essential medium (Wuhan Servicebio Technology Co., Ltd.) supplemented with 10% fetal bovine serum (Cellmax) and 1%

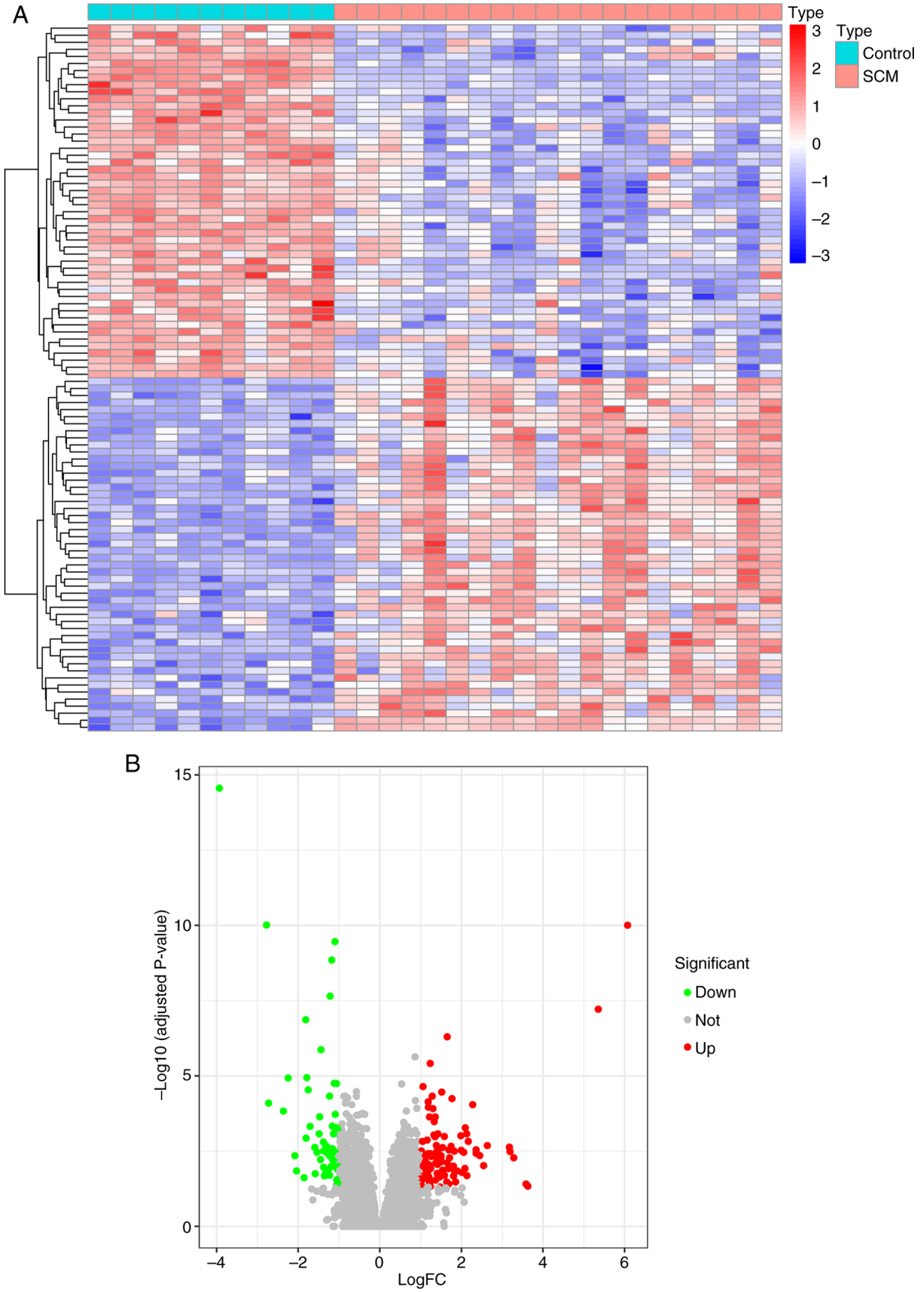

Figure 2. Screening of DEGs. (A) Heatmap of DEGs in GSE79962, the expression of genes from low to high is shown in blue to red. (B) Volcano plot of DEGs in GSE79962. Green dots represent significantly down-regulated genes. Red dots represent significantly up-regulated genes. Gray dots represent genes with no significant differential expression. DEGs, differentially expressed genes; FC, fold change.

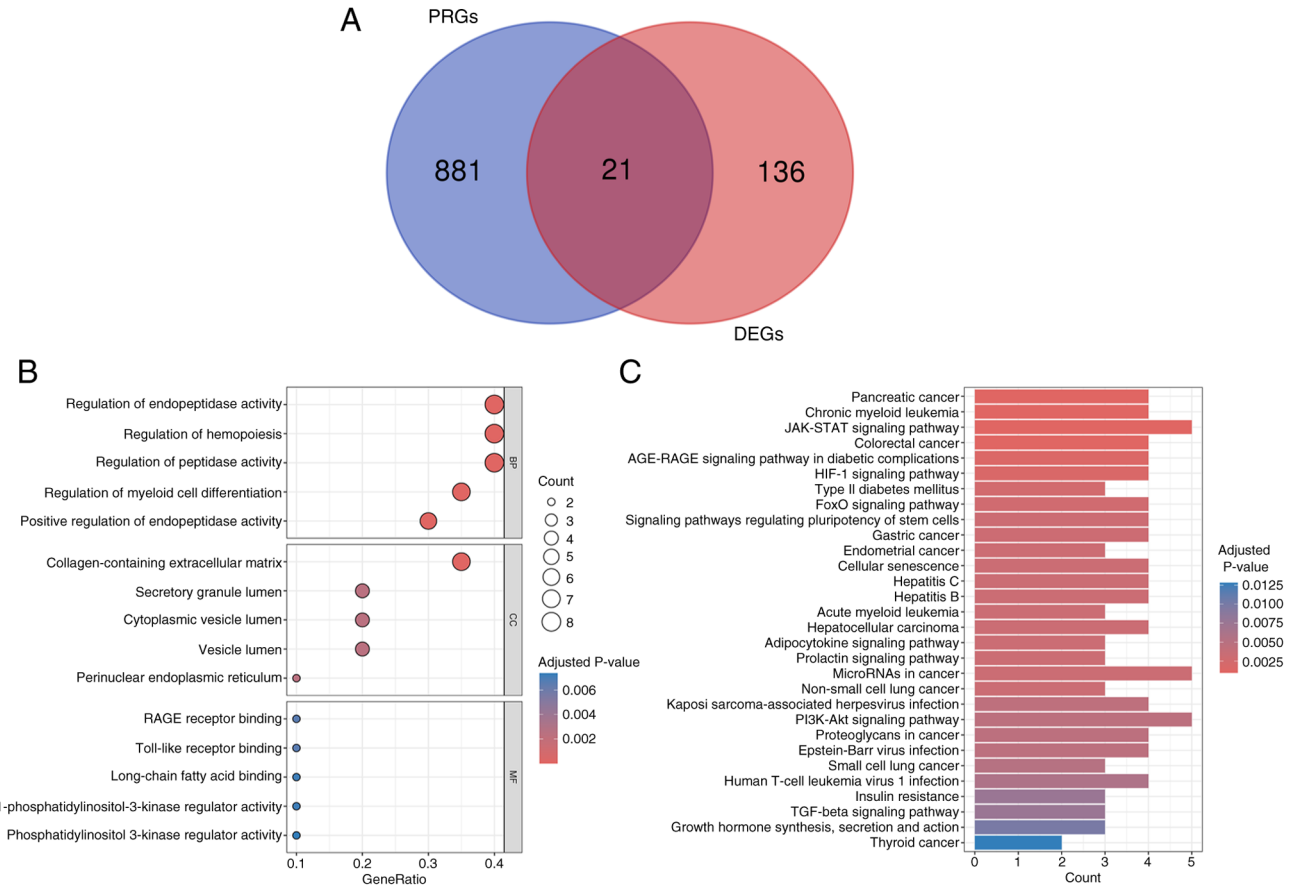

Figure 3. Identification of differentially expressed PRGs and GO/KEGG enrichment analysis. (A) Venn diagrams were used to show genes where DEGs intersected with PRGs. (B) Differentially expressed PRGs were used for GO analysis. The top five functional terms in the categories biological process, cellular component and molecular function were visualized using bubble plots. Larger bubbles indicate a higher number of enriched genes. (C) The top 30 KEGG pathways of differentially expressed PRGs were shown using bar plots. A redder color indicates a higher enrichment significance. PRGs, PANoptosis-related genes; GO, Gene Ontology; KEGG, Kyoto Encyclopedia of Genes and Genomes; DEGs, differentially expressed genes.

penicillin-streptomycin antibiotics (NCM Biotech) in an incubator with 5% CO_2 at 37˚C. To mimic SCM, cardiomyocytes were treated with 10 μg/ml LPS (MilliporeSigma) for 12 h at 37˚C.

Reverse transcription quantitative PCR (qPCR). Total RNA from cells was extracted using RNA extraction solution (Wuhan Servicebio Technology Co., Ltd.) according to the manufacturer's instructions. cDNA synthesis was performed using a reverse transcription kit (TransGen Biotech Co., Ltd.). The conditions for reverse transcription were 42˚C for 15 min and then 85˚C for 5 sec. The qPCR was carried out on a Roche Light Cycler 96 Real-Time System (Roche Diagnostics GmbH) using PerfectStart® Green qPCR SuperMix (TransGen Biotech Co., Ltd.). The qPCR was performed with an initial denaturation at 94˚C for 30 sec, followed by 40 cycles of 5 sec at 94˚C and 30 sec at 60˚C. The following primers were used: GADD45B forward, 5'-TGCCTCCTGGTCACG AACTG-3' and reverse, 5'-CCATTGGTTATTGCCTCTGCT CTC-3'; RIPK2 forward, 5'-TCGTGTTCCTTGGCTGTAATA AGTC-3' and reverse, 5'-CATCTGGCTCACAATGGCTTC C-3'; and β-actin forward, 5'-CTATTGGCAACGAGCGGT TCC-3' and reverse, 5'-GCACTGTGTTGGCATAGAGGT C-3'. The relative gene expression was calculated using the $2^{-\Delta\Delta Cq}$ method (45).

Statistical analysis. Analysis of two data groups was conducted utilizing either Student's t-test or the Wilcoxon rank-sum test, as appropriate. R software (version 4.3.1; RStudio, Inc.) and GraphPad Prism version 9 (Dotmatics) were used for analysis and plotting. $P<0.05$ was considered to indicate a statistically significant difference.

Results

Screening of DEGs. The flowchart of the present study is shown in Fig. 1. A total of 31 samples from the GSE79962 dataset were included in the present study. The SCM group included 20 samples, and the control group included 11 samples. A total of 157 DEGs, including 59 downregulated genes and 98 upregulated genes, were obtained using the 'limma' R package. DEGs are presented in heatmaps (Fig. 2A) and volcano plots (Fig. 2B), and the top 50 differentially expressed up- and downregulated genes are shown in the heatmap.

Differentially expressed PRGs and GO/KEGG enrichment analysis. A total of 21 differentially expressed PRGs were identified by intersecting 157 DEGs with 902 PRGs, and the results are displayed in the Venn diagram (Fig. 3A). To investigate the potential biological functions of the differentially expressed PRGs, these 21 genes were subjected to GO

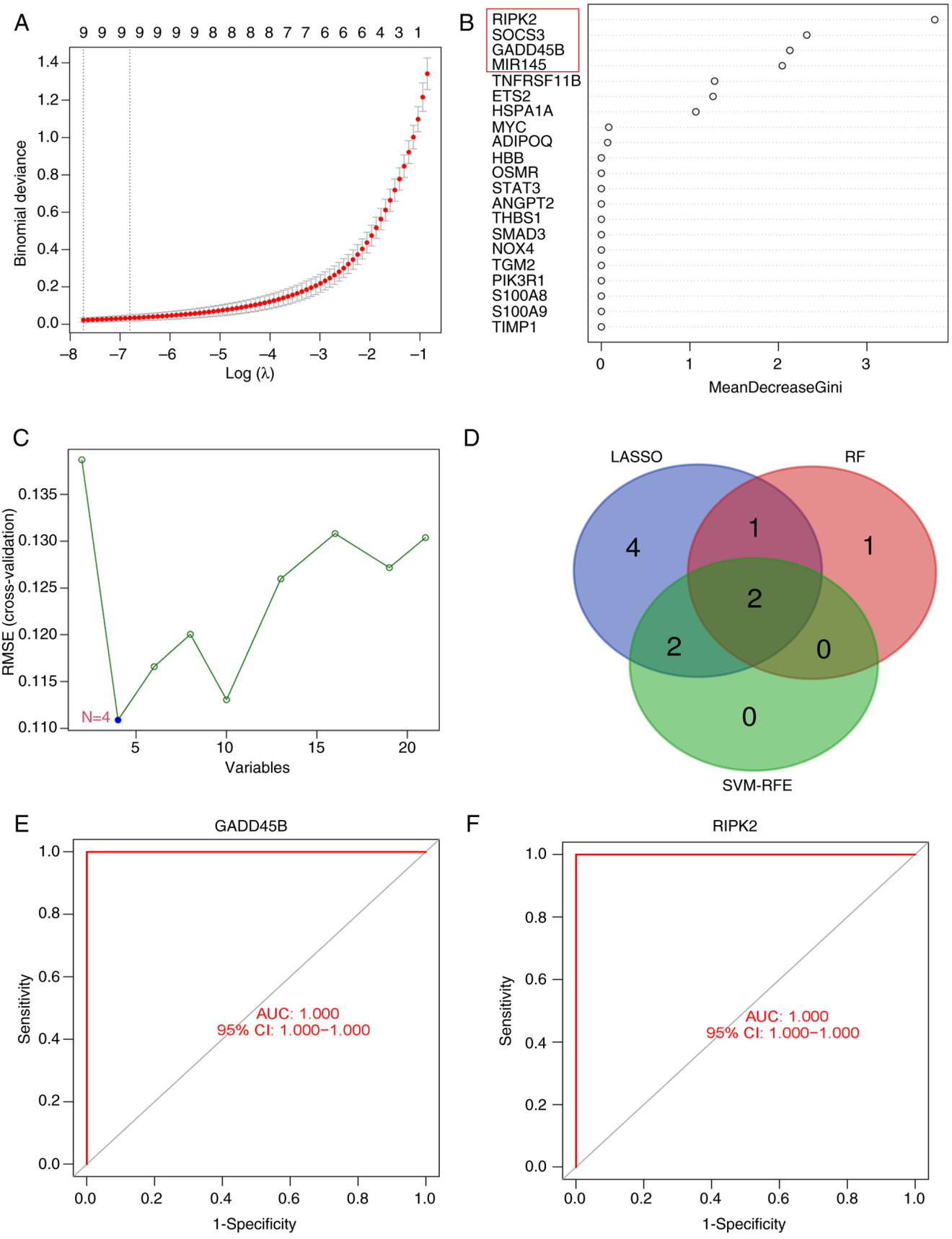

Figure 4. Identification of key genes by three machine learning algorithms and evaluation of the diagnostic value of key genes. (A) Nine differentially expressed PRGs were obtained using LASSO regression analysis. (B) Four differentially expressed PRGs were obtained using the RF algorithm (indicated by the red box). (C) Four differentially expressed PRGs were obtained using the SVM-RFE algorithm. (D) The two key genes (RIPK2 and GADD45B) were obtained by intersecting the results of LASSO regression, RF and SVM-RFE. The Venn diagram showed the results of the intersection. (E and F) Receiver operating characteristic curves were used to assess the diagnostic efficacy of key genes (E) GADD45B and (F) RIPK2. PRGs, PANoptosis-related genes; LASSO, least absolute shrinkage and selection operator; RF, random forest; SVM-RFE, support vector machine-recursive feature elimination; AUC, area under the curve; CI, confidence interval; RMSE, root mean square error.

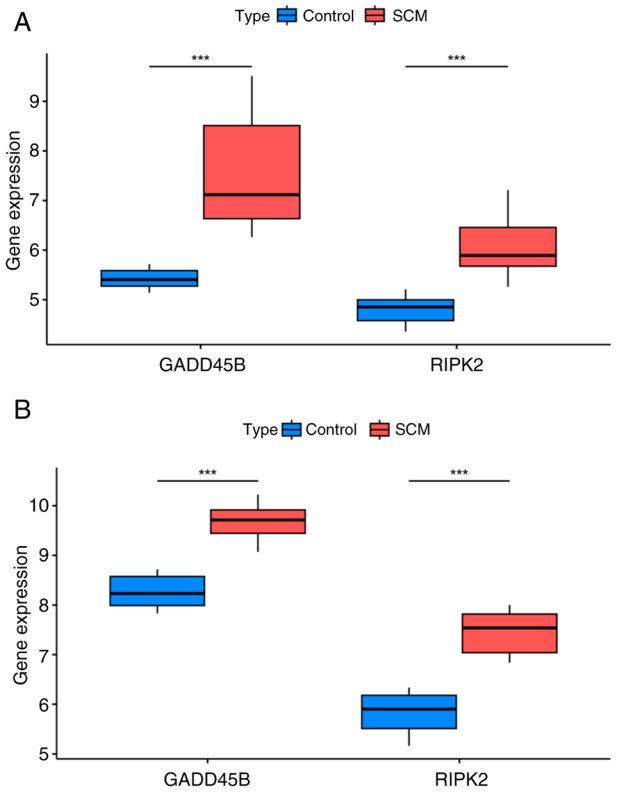

Figure 5. External dataset validation of key gene expression. (A) Comparison of key gene expression between the control group and the SCM group in the GSE79962 dataset. (B) In the validation set (combined from GSE53007 and GSE142615), the comparison of the expression of key genes between the control group and the SCM group. The above results were presented in box plots. ***P<0.001. SCM, septic cardiomyopathy.

and KEGG enrichment analyses. The top five BPs, CCs and MFs were shown using a bubble diagram (Fig. 3B). The top 5 relevant BP terms were 'regulation of endopeptidase activity', 'regulation of hemopoiesis', 'regulation of peptidase activity', 'regulation of myeloid cell differentiation' and 'positive regulation of endopeptidase activity'. The top 5 relevant CC terms were 'collagen-containing extracellular matrix', 'secretory granule lumen', 'cytoplasmic vesicle lumen', 'vesicle lumen' and 'perinuclear endoplasmic reticulum'. The top 5 relevant MF terms were 'RAGE receptor binding', 'Toll-like receptor binding', 'long-chain fatty acid binding', '1-phosphatidylinositol-3-kinase regulator activity' and 'phosphatidylinositol 3-kinase regulator activity'. The top 30 KEGG pathways are presented using a bar plot, and these KEGG pathways included 'JAK-STAT signaling pathway', 'PI3K-Akt signaling pathway' and 'HIF-1 signaling pathway' (Fig. 3C).

Identification of key genes and diagnostic value assessment. To further mine key genes for SCM, three machine learning algorithms were used to evaluate the 21 differentially expressed PRGs: Nine candidate key genes were screened by LASSO regression analysis (Fig. 4A); the RF algorithm identified four candidate key genes with importance scores >2 (Fig. 4B); and the SVM-RFE algorithm identified four candidate key genes (Fig. 4C). Two key genes were identified on the basis of the results of three algorithms (Fig. 4D), and these genes were GADD45B and RIPK2. These findings suggested that GADD45B and RIPK2 may play important roles in SCM. Additionally, to explore the diagnostic ability of these two key genes for SCM, ROC curves were plotted and the AUC values of GADD45B and RIPK2 were both 1.00 (Fig. 4E and F). The results indicated that both key genes had superior diagnostic abilities.

External dataset validation of GADD45B and RIPK2 expression. In the GSE79962 dataset, the levels of GADD45B and RIPK2 were significantly elevated in the SCM group (Fig. 5A); in the validation set, GADD45B with RIPK2 remained highly expressed in the SCM group (Fig. 5B). The aforementioned results were consistent and all the differences were statistically significant. These results suggested that the expression of GADD45B and RIPK2 is elevated in the myocardial tissues of both SCM patients and SCM mice compared with their respective controls.

Assessment of immune cell infiltration and correlation of key genes with immune cells. The CIBERSORT algorithm was used to analyze the relative abundance of different immune cell types across the 31 samples in the GSE79962 dataset. The bar-plot diagram shows the proportions of 22 immune cell types in each sample (Fig. 6A). The expression level of GADD45B was positively correlated with the proportions of naive B cells and neutrophils; conversely, the expression level of GADD45B was inversely related to the proportion of mast cells resting (Fig. 6B). The expression level of RIPK2 showed a positive relationship with the proportion of neutrophils (Fig. 6C). The findings of the immune infiltration analysis indicated that RIPK2 and GADD45B may be involved in regulating immune cell infiltration in SCM.

Single-gene GSEA analysis of GADD45B and RIPK2. To further explore the possible molecular mechanisms associated with key PRGs in SCM, single-gene GSEA was conducted. The findings indicated that pathways enriched in the high GADD45B expression group were predominantly 'IL-17 signaling pathway', 'malaria', 'proteasome', 'ribosome biogenesis in eukaryotes' and 'TNF signaling pathway' (Fig. 7A). Pathways enriched in the low GADD45B expression group were primarily the 'drug metabolism-cytochrome P450', 'ether lipid metabolism', '*Staphylococcus aureus* infection', 'systemic lupus erythematosus' and 'taurine and hypotaurine metabolism' (Fig. 7B). In addition, pathways enriched in the high RIPK2 expression group were mainly 'African trypanosomiasis', 'IL-17 signaling pathway', 'malaria', 'ribosome biogenesis in eukaryotes' and 'TNF signaling pathway' (Fig. 7C). On the other hand, pathways enriched in the low RIPK2 expression group were mainly '2-oxocarboxylic acid metabolism', 'carbohydrate digestion and absorption', 'gap junction', 'glucagon signaling pathway' and 'insulin secretion' (Fig. 7D).

GADD45B- and RIPK2-based ceRNA network and potential therapeutic agents for SCM. To further explore gene functions and regulatory mechanisms, a ceRNA regulatory network was constructed. Eight miRNAs and 16 lncRNAs were found to be associated with the key genes and were visualized using Cytoscape (Fig. 8A). To explore potential

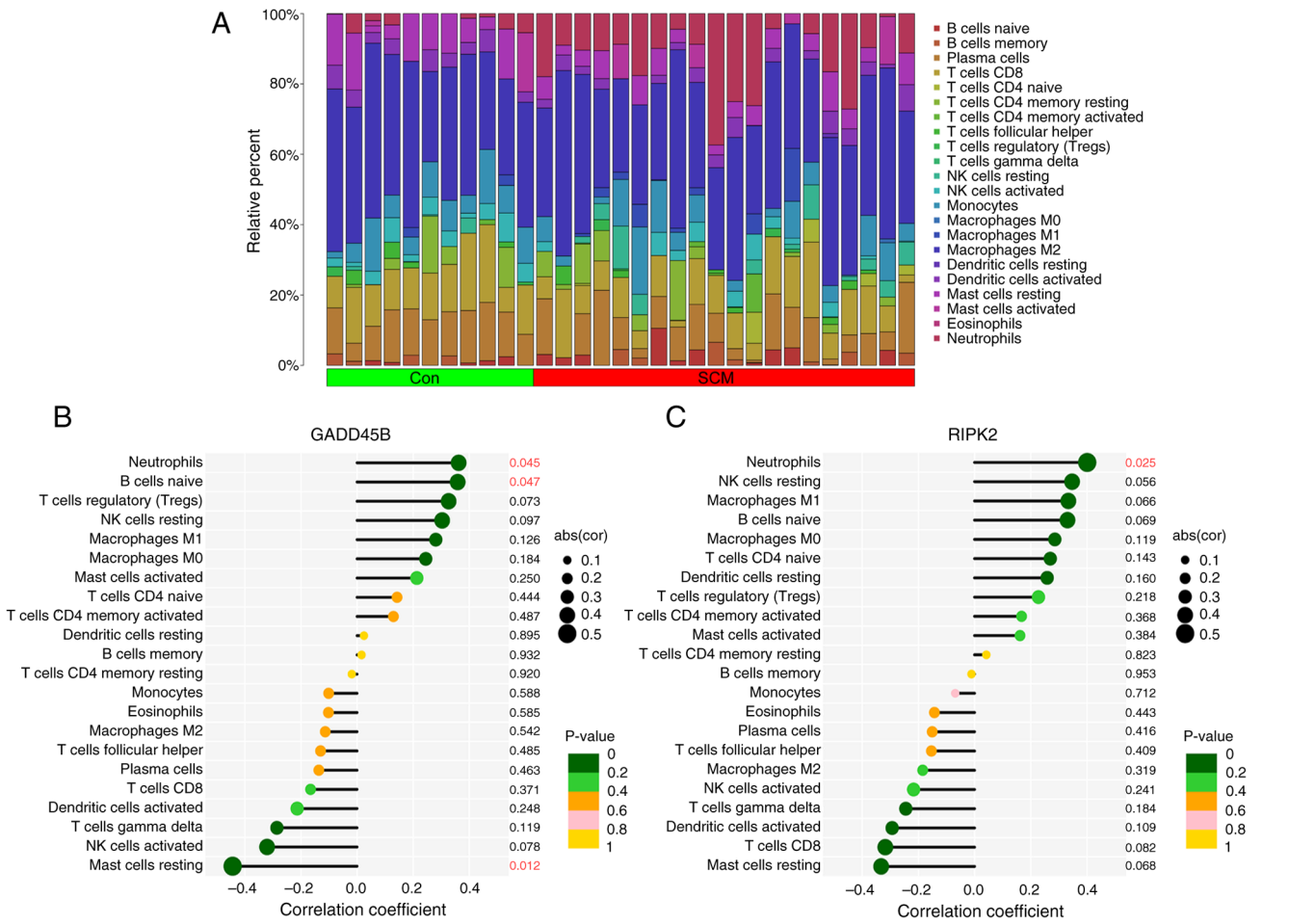

Figure 6. Assessment of immune cell infiltration and correlation of key genes with immune cells. (A) A bar-plot diagram was used to show the percentage of 22 immune cell types in each sample. Each color represents the corresponding type of cell. (B) A lollipop plot was used to show the correlation between GADD45B and the 22 immune cell types. (C) A lollipop plot was used to show the correlation between RIPK2 and the 22 immune cell types. The size of the dots reflects the strength of the correlation. Con, control; SCM, septic cardiomyopathy; abs(cor), absolute value of correlation coefficient.

therapeutic agents for SCM, the DGIDB database was used to obtain drugs associated with the key genes; the results showed that 10 drugs or molecular compounds were related to RIPK2, whereas no drugs related to GADD45B were found (Fig. 8B). Among the 10 drugs or molecular compounds related to RIPK2, the five with the highest interaction scores were OD36, SRC kinase inhibitor I, RIPK2 inhibitor 8, GSK583 and RIPK2 inhibitor 5.

Experimental validation of GADD45B and RIPK2 expression. The LPS-induced HL-1 cell injury model was used to explore the expression levels of the key PRGs. As hypothesized, the mRNA expression levels of GADD45B and RIPK2 were significantly elevated in the LPS-induced HL-1 cell injury group compared with the control group (Fig. 9A and B). This was consistent with the previous bioinformatics analyses.

Discussion

Previously published data have shown that the prevalence of sepsis is increasing worldwide (46). Sepsis typically leads to myocardial damage and the mortality rate of septic patients with cardiac dysfunction is notably high. The illness compromises both the physical and mental well-being of the patient, while simultaneously imposing a notable strain on families and society, and there are currently limited treatment options available for patients with SCM. Research indicates that the development of SCM involves various forms of cell death, including apoptosis, autophagy and ferroptosis (47,48). To the best of our knowledge, there are few studies focused on the role of PANoptosis, a new type of programmed cell death, and its association in SCM. In the present study, two key PRGs potentially associated with the progression of SCM were identified using bioinformatics analysis and machine learning techniques. The findings suggested that PANoptosis may be associated with the development of SCM.

In the present study, 157 DEGs were screened in the SCM group compared with the control group, and 21 differentially expressed PRGs were obtained by intersecting these 157 DEGs with PANoptosis-related genes. The functional enrichment analysis indicated that the 21 differentially expressed PRGs were involved primarily in the 'regulation of endopeptidase activity', 'toll-like receptor binding', 'JAK-STAT signaling pathway' and 'PI3K-Akt signaling pathway'. According to previous studies, these enrichment results are strongly associated with SCM. For instance, it has been shown that apoptosis and inflammation are improved by regulating JAK2/STAT6 in an LPS-induced myocardial injury model (10). Another

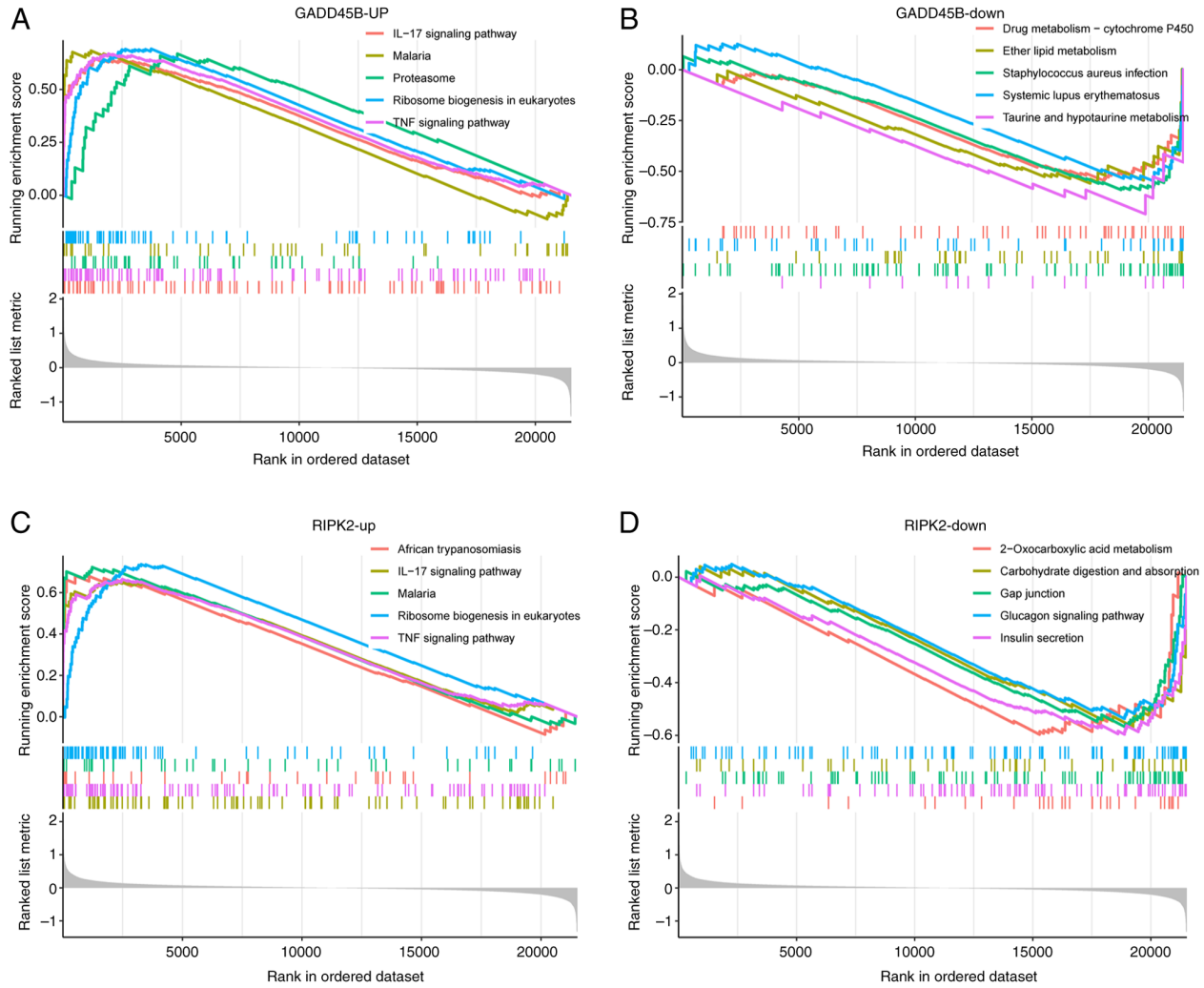

Figure 7. GSEA analysis of key genes. (A and B) GSEA analysis of (A) GADD45B-up and (B) GADD45B-down. (C and D) GSEA analysis of (C) RIPK2-up and (D) RIPK2-down. Enrichment plots were used to display the five most significantly upregulated or downregulated pathways. GSEA, gene set enrichment analysis.

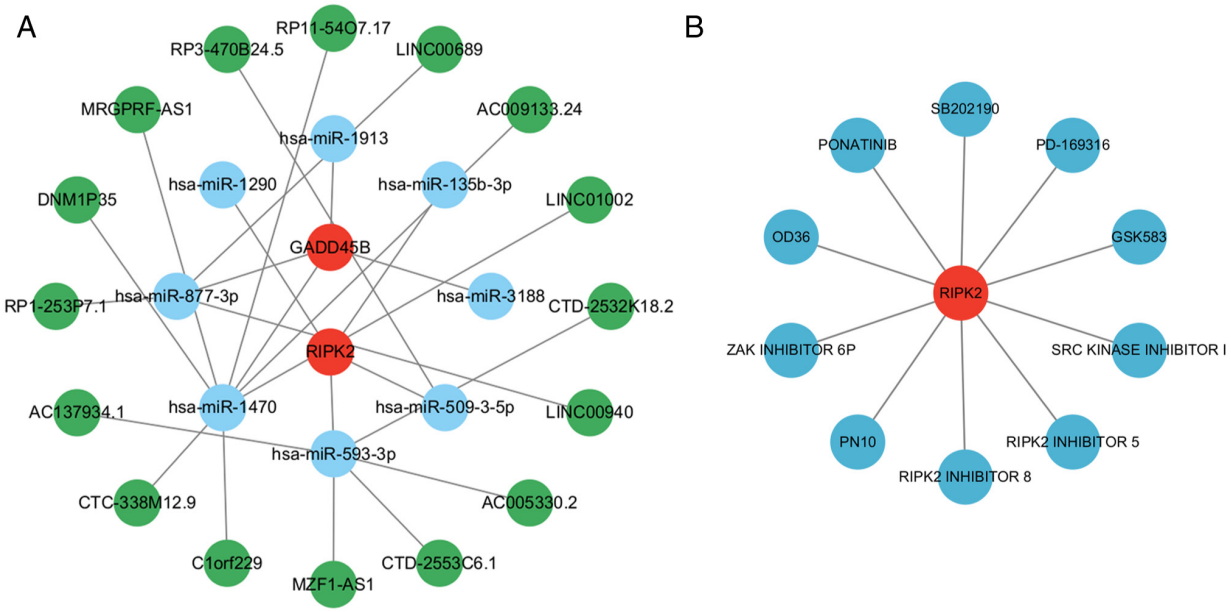

Figure 8. Key gene-based ceRNA regulatory networks and potential therapeutic agents. (A) Construction of ceRNA networks based on key genes. The ceRNA network consists of two mRNAs, eight miRs and 16 long non-coding RNAs. (B) Potential drug prediction based on key genes. 10 drugs or molecular compounds related to RIPK2 were obtained from the Drug-Gene Interaction Database. ceRNA, competitive endogenous RNA. miR, microRNA.

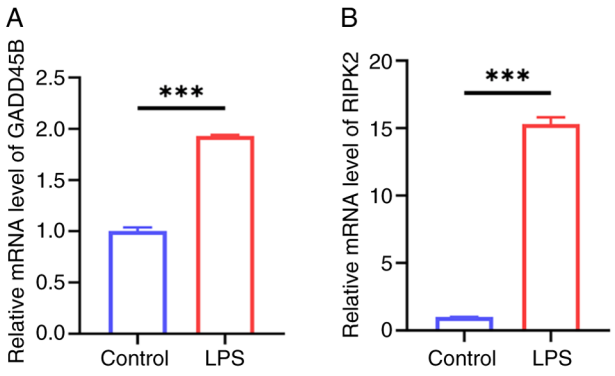

Figure 9. Reverse transcription quantitative PCR to verify the expression of key PRGs. (A) Comparison of GADD45B expression in the control and LPS-induced HL-1 cell injury group. (B) Comparison of RIPK2 expression in the control and LPS-induced HL-1 cell injury group. ***P<0.001. PRGs, PANoptosis-related genes; LPS, lipopolysaccharide.

study demonstrated that modulation of the PI3K-Akt signaling pathway can alleviate LPS-induced cardiomyocyte apoptosis (49). In addition, LASSO regression, RF and SVM-RFE were used to further screen 2 key PRGs, GADD45B and RIPK2, involved in the pathogenesis of SCM. The AUC values for both key genes were 1, suggesting that both GADD45B and RIPK2 have high diagnostic value.

GADD45B belongs to the GADD45 family, a group that plays a role in regulating apoptosis and cellular proliferation (50), and previous studies on GADD45B have focused on tumors, stroke and kidney injury (50-52). In cardiovascular diseases, ischemia/hypoxia-induced cardiomyocyte apoptosis can be markedly attenuated by downregulation of GADD45B, suggesting that GADD45B plays a key role in cardiomyocyte apoptosis (53). Additionally, earlier research has reported elevated expression of GADD45B in the myocardium of diabetic mice compared with controls, with further increases observed in myocardial ischemia/reperfusion in diabetic mice (54). In the present study, the expression level of GADD45B was elevated in the SCM group, and it was also found to be elevated in the LPS-induced cardiomyocyte model. However, to the best of our knowledge, no study has yet identified a role for GADD45B in SCM and further research is required to elucidate its role.

RIPK2 is a member of the RIP family, of which members of the family have been reported to have serine/threonine kinase activity; additionally, RIPK2 has tyrosine kinase activity (55). Previous studies have found that RIPK2 is involved mainly in gene transcription regulation, inflammation, autophagy and apoptosis (56). Current studies on RIPK2 are related mainly to tumors, autoimmune diseases and inflammation-related diseases (57-59), and there are fewer studies related to RIPK2 and cardiovascular disease. One study showed that RIPK2 knockdown ameliorated cardiac hypertrophy in pressure-overloaded mice (60); this finding highlights that RIPK2 could serve as a promising target for addressing myocardial hypertrophy or heart failure. A different investigation revealed that RIPK2 deficiency in a mouse model of myocardial ischemia led to a notable decline in cardiac function (61); therefore, these findings suggest that RIPK2 is expected to be a new effective target in ischemic heart disease. In the present study, it was observed that RIPK2 expression was elevated in SCM, and as RIPK2 is closely related to inflammation and apoptosis, it was hypothesized that RIPK2 may be associated with the development of SCM.

An immune infiltration analysis was performed, which revealed that the proportion of neutrophils in the SCM group was notably greater than that in the control group. A previous study has also demonstrated marked neutrophil infiltration in the myocardium of SCM mice (62). Neutrophils play a dual role in sepsis, and while they effectively eliminate pathogens, overactivated neutrophils can also exacerbate tissue damage (63). During sepsis, neutrophils release large amounts of reactive oxygen species and proteolytic enzymes, thereby exacerbating the inflammatory response; therefore, inhibiting excessive neutrophil infiltration is a potential therapeutic approach for SCM. Pretreatment with the ferroptosis inhibitor ferrostatin-1 notably suppressed neutrophil infiltration in the myocardium and reduced the expression of myocardial inflammatory cytokines after cecal ligation and puncture in mice (64). Additionally, a correlation analysis was conducted between key genes and 22 types of immune cells, and the findings revealed a significant correlation between the expression of both key genes and the percentage of neutrophils. A more detailed exploration of the connections between key PRGs and immune cells may be critical for the treatment of SCM.

To understand the related pathways and molecular functions of key genes, single-gene GSEA was performed in the current study. The results revealed that both GADD45B and RIPK2 show a significant correlation with the upregulation of gene sets related to the 'IL-17 signaling pathway' and 'TNF signaling pathway'. These findings are consistent with previous research; for instance, in a mouse model of acute pancreatitis induced by hypertriglyceridemia, knockdown of GADD45B markedly attenuated the serum levels of pro-inflammatory cytokines IL-6 and TNF-α (65). In another study, it was found that RIPK2 knockdown could enhance the cytosolic level of IKBα, block p65 nuclear translocation and inhibit the expression of TNF-α and IL-17 in an ovalbumin-induced mouse asthma model (66). These studies suggest that knockdown of GADD45B and RIPK2 can suppress the progression of certain diseases by inhibiting inflammation. The pathogenesis of SCM is closely related to excessive inflammatory responses, and in SCM, both the TNF-α pathway and the IL-17 pathway play important roles in the inflammatory response (67,68), and their synergistic action can amplify the inflammatory reaction (69). This may further exacerbate the inflammatory response in cardiomyocytes; therefore, an investigation into the roles and mechanisms of GADD45B and RIPK2 in inflammation will facilitate the development of novel therapeutic approaches for SCM.

In the present study, a ceRNA regulatory network was constructed that comprises two mRNAs, eight miRNAs and 16 lncRNAs. It has been suggested that miR-1290 may be associated with sepsis and associated lung injury (70), whereas another study on miR-1290 showed that increasing the level of miR-1290 in cardiomyocytes reduced apoptosis under hypoxic conditions (71). The ceRNA regulatory network provides promising targets for the treatment of SCM, but further experimental studies are required. Additionally, drugs or chemical compounds associated with key genes were

obtained through the DGIDB database. The results showed that there were 10 drugs or chemical compounds related to RIPK2, whereas no drugs or chemical compounds related to GADD45B were found. Among these 10 drugs or chemical compounds, OD36, a RIPK2 inhibitor, has been reported to reduce neutrophil and lymphocyte infiltration in the peritoneal cavity of mice with peritonitis (72). However, to the best of our knowledge, no studies have reported the application of OD36 in SCM. This finding indicates that there is still notable room for improvement in the treatment of SCM.

To the best of our knowledge, the present study was the first to explore the role of PANoptosis in SCM, which provides a theoretical basis for subsequent related studies. However, there are certain limitations. First, a small sample size was used and more samples need to be included in subsequent studies. Second, it is essential to conduct both *in vivo* and *in vitro* experiments to confirm the function of key PRGs in SCM. Finally, due to the lack of complete information, it was not possible to compare the baseline populations between the SCM group and the healthy control group. In the future, it is the aim to explore the pathogenesis of SCM further, hoping to provide more options for SCM treatment.

In conclusion, in the present study, two key PRGs, RIPK2 and GADD45B, were screened through bioinformatics and machine learning. Both genes demonstrated good diagnostic capabilities for SCM. In addition, these genes may play a role in SCM by regulating certain immune cells. Finally, a novel theoretical foundation for the treatment of SCM was established by constructing a ceRNA regulatory network and a drug-gene interaction network.

Acknowledgements

Not applicable.

Funding

No funding was received.

Availability of data and materials

Data related to this study are available from the GEO database, including GSE79962, GSE53007 and GSE142615 (https://www.ncbi.nlm.nih.gov/geo/). The data generated in the present study may be requested from the corresponding author.

Authors' contributions

QT, ZZ and YY contributed to the overall design of the research. PY and JZ collected the relevant data. PY and YY performed the data analysis. YY and JZ conducted the experiments. YY and JZ wrote the original draft. QT and ZZ edited the manuscript. QT, ZZ and YY revised the manuscript. All authors read and approved the final version of the manuscript. YY and QT confirm the authenticity of all the raw data.

Ethics approval and consent to participate

Not applicable.

Patient consent for publication

Not applicable.

Competing interests

The authors declare that they have no competing interests.

References

1. Zhang YY and Ning BT: Signaling pathways and intervention therapies in sepsis. Signal Transduct Target Ther 6: 407, 2021.
2. Fleischmann-Struzek C and Rudd K: Challenges of assessing the burden of sepsis. Med Klin Intensivmed Notfmed 118 (Suppl 2): S68-S74, 2023.
3. Zaky A, Deem S, Bendjelid K and Treggiari MM: Characterization of cardiac dysfunction in sepsis: An ongoing challenge. Shock 41: 12-24, 2014.
4. Hollenberg SM: Sepsis-associated cardiomyopathy: Long-term prognosis, management, and Guideline-directed medical therapy. Curr Cardiol Rep 27: 5, 2025.
5. Hasegawa D, Ishisaka Y, Maeda T, Prasitlumkum N, Nishida K, Dugar S and Sato R: Prevalence and prognosis of Sepsis-induced cardiomyopathy: A systematic review and Meta-analysis. J Intensive Care Med 38: 797-808, 2023.
6. Li Y, Ge S, Peng Y and Chen X: Inflammation and cardiac dysfunction during sepsis, muscular dystrophy, and myocarditis. Burns Trauma 1: 109-121, 2013.
7. Dickson K and Lehmann C: Inflammatory response to different toxins in experimental sepsis models. Int J Mol Sci 20: 4341, 2019.
8. van der Slikke EC, Star BS, van Meurs M, Henning RH, Moser J and Bouma HR: Sepsis is associated with mitochondrial DNA damage and a reduced mitochondrial mass in the kidney of patients with sepsis-AKI. Crit Care 25: 36, 2021.
9. Oliveira F, Assreuy J and Sordi R: The role of nitric oxide in sepsis-associated kidney injury. Biosci Rep 42: BSR20220093, 2022.
10. Jiang L, Zhang L, Yang J, Shi H, Zhu H, Zhai M, Lu L, Wang X, Li XY, Yu S, *et al*: 1-Deoxynojirimycin attenuates septic cardiomyopathy by regulating oxidative stress, apoptosis, and inflammation via the JAK2/STAT6 signaling pathway. Biomed Pharmacother 155: 113648, 2022.
11. Malireddi RKS, Kesavardhana S and Kanneganti TD: ZBP1 and TAK1: Master Regulators of NLRP3 Inflammasome/Pyroptosis, Apoptosis, and Necroptosis (PAN-optosis). Front Cell Infect Microbiol 9: 406, 2019.
12. Christgen S, Tweedell RE and Kanneganti TD: Programming inflammatory cell death for therapy. Pharmacol Ther 232: 108010, 2022.
13. Zhu P, Ke ZR, Chen JX, Li SJ, Ma TL and Fan XL: Advances in mechanism and regulation of PANoptosis: Prospects in disease treatment. Front Immunol 14: 1120034, 2023.
14. He YQ, Deng JL, Zhou CC, Jiang SG, Zhang F, Tao X and Chen WS: Ursodeoxycholic acid alleviates sepsis-induced lung injury by blocking PANoptosis via STING pathway. Int Immunopharmacol 125: 111161, 2023.
15. Zhou R, Ying J, Qiu X, Yu L, Yue Y, Liu Q, Shi J, Li X, Qu Y and Mu D: A new cell death program regulated by toll-like receptor 9 through p38 mitogen-activated protein kinase signaling pathway in a neonatal rat model with sepsis associated encephalopathy. Chin Med J (Engl) 135: 1474-1485, 2022.
16. Matkovich SJ, Al Khiami B, Efimov IR, Evans S, Vader J, Jain A, Brownstein BH, Hotchkiss RS and Mann DL: Widespread Down-regulation of cardiac mitochondrial and sarcomeric genes in patients with sepsis. Crit Care Med 45: 407-414, 2017.
17. Zhu H, Wu J, Li C, Zeng Z, He T, Liu X, Wang Q, Hu X, Lu Z and Cai H: Transcriptome analysis reveals the mechanism of pyroptosis-related genes in septic cardiomyopathy. PeerJ 11: e16214, 2023.
18. Shi Y, Zheng X, Zheng M, Wang L, Chen Y and Shen Y: Identification of mitochondrial function-associated lncRNAs in septic mice myocardium. J Cell Biochem 122: 53-68, 2021.
19. Ritchie ME, Phipson B, Wu D, Hu Y, Law CW, Shi W and Smyth GK: limma powers differential expression analyses for RNA-sequencing and microarray studies. Nucleic Acids Res 43: e47, 2015.

20. Gustavsson EK, Zhang D, Reynolds RH, Garcia-Ruiz S and Ryten M: ggtranscript: An R package for the visualization and interpretation of transcript isoforms using ggplot2. Bioinformatics 38: 3844-3846, 2022.
21. Zhang X, Chao P, Zhang L, Xu L, Cui X, Wang S, Wusiman M, Jiang H and Lu C: Single-cell RNA and transcriptome sequencing profiles identify immune-associated key genes in the development of diabetic kidney disease. Front Immunol 14: 1030198, 2023.
22. Sun W, Li P, Wang M, Xu Y, Shen D, Zhang X and Liu Y: Molecular characterization of PANoptosis-related genes with features of immune dysregulation in systemic lupus erythematosus. Clin Immunol 253: 109660, 2023.
23. The Gene Ontology Consortium: The gene ontology resource: 20 years and still GOing strong. Nucleic Acids Res 47: D330-D338, 2019.
24. Kanehisa M and Goto S: KEGG: Kyoto encyclopedia of genes and genomes. Nucleic Acids Res 28: 27-30, 2000.
25. Wu T, Hu E, Xu S, Chen M, Guo P, Dai Z, Feng T, Zhou L, Tang W, Zhan L, *et al*: clusterProfiler 4.0: A universal enrichment tool for interpreting omics data. Innovation (Camb) 2: 100141, 2021.
26. Li Y, Yu J, Li R, Zhou H and Chang X: New insights into the role of mitochondrial metabolic dysregulation and immune infiltration in septic cardiomyopathy by integrated bioinformatics analysis and experimental validation. Cell Mol Biol Lett 29: 21, 2024.
27. Chen G, Qi H, Jiang L, Sun S, Zhang J, Yu J, Liu F, Zhang Y and Du S: Integrating single-cell RNA-Seq and machine learning to dissect tryptophan metabolism in ulcerative colitis. J Transl Med 22: 1121, 2024.
28. Engebretsen S and Bohlin J: Statistical predictions with glmnet. Clin Epigenetics 11: 123, 2019.
29. Wang Q and Liu X: Screening of feature genes in distinguishing different types of breast cancer using support vector machine. Onco Targets Ther 8: 2311-2317, 2015.
30. Kuhn M: Building predictive models in R using the caret package. J Stat Software 28: 1-26, 2008.
31. Scharl T, Grü B and Leisch F: Mixtures of regression models for time course gene expression data: Evaluation of initialization and random effects. Bioinformatics 26: 370-377, 2010.
32. Alderden J, Pepper GA, Wilson A, Whitney JD, Richardson S, Butcher R, Jo Y and Cummins MR: Predicting pressure injury in critical care patients: A Machine-learning model. Am J Crit Care 27: 461-468, 2018.
33. Robin X, Turck N, Hainard A, Tiberti N, Lisacek F, Sanchez JC and Müller M: pROC: An open-source package for R and S+ to analyze and compare ROC curves. BMC Bioinformatics 12: 77, 2011.
34. Li J, Zhang Y, Lu T, Liang R, Wu Z, Liu M, Qin L, Chen H, Yan X, Deng S, *et al*: Identification of diagnostic genes for both Alzheimer's disease and Metabolic syndrome by the machine learning algorithm. Front Immunol 13: 1037318, 2022.
35. Zhang WY, Chen ZH, An XX, Li H, Zhang HL, Wu SJ, Guo YQ, Zhang K, Zeng CL and Fang XM: Analysis and validation of diagnostic biomarkers and immune cell infiltration characteristics in pediatric sepsis by integrating bioinformatics and machine learning. World J Pediatr 19: 1094-1103, 2023.
36. Newman AM, Liu CL, Green MR, Gentles AJ, Feng W, Xu Y, Hoang CD, Diehn M and Alizadeh AA: Robust enumeration of cell subsets from tissue expression profiles. Nat Methods 12: 453-457, 2015.
37. Peng H, Hu Q, Zhang X, Huang J, Luo S, Zhang Y, Jiang B and Sun D: Identifying therapeutic targets and potential drugs for diabetic retinopathy: Focus on oxidative stress and immune infiltration. J Inflamm Res 18: 2205-2227, 2025.
38. Zheng Z, Li K, Yang Z, Wang X, Shen C, Zhang Y, Lu H, Yin Z, Sha M, Ye J and Zhu L: Transcriptomic analysis reveals molecular characterization and immune landscape of PANoptosis-related genes in atherosclerosis. Inflamm Res 73: 961-678, 2024.
39. Huang X, Liu J and Huang W: Identification of S100A8 as a common diagnostic biomarkers and exploring potential pathogenesis for osteoarthritis and metabolic syndrome. Front Immunol 14: 1185275, 2023.
40. John B, Enright AJ, Aravin A, Tuschl T, Sander C and Marks DS: Human MicroRNA targets. PLoS Biol 2: e363, 2004.
41. Chen Y and Wang X: miRDB: An online database for prediction of functional microRNA targets. Nucleic Acids Res 48: D127-D131, 2020.
42. Sticht C, De La Torre C, Parveen A and Gretz N: miRWalk: An online resource for prediction of microRNA binding sites. PLoS One 13: e0206239, 2018.
43. Lewis BP, Burge CB and Bartel DP: Conserved seed pairing, often flanked by adenosines, indicates that thousands of human genes are microRNA targets. Cell 120: 15-20, 2005.
44. Furió-Tarí P, Tarazona S, Gabaldón T, Enright AJ and Conesa A: spongeScan: A web for detecting microRNA binding elements in lncRNA sequences. Nucleic Acids Res 44: W176-W180, 2016.
45. Livak KJ and Schmittgen TD: Analysis of relative gene expression data using real-time quantitative PCR and the 2(-Delta Delta C(T)) method. Methods 25: 402-408, 2001.
46. Deutschman CS and Tracey KJ: Sepsis: Current dogma and new perspectives. Immunity 40: 463-475, 2014.
47. Lu JS, Wang JH, Han K and Li N: Nicorandil regulates ferroptosis and mitigates septic cardiomyopathy via TLR4/SLC7A11 signaling pathway. Inflammation 47: 975-988, 2024.
48. Yuan X, Chen G, Guo D, Xu L and Gu Y: Polydatin alleviates septic myocardial injury by promoting SIRT6-Mediated autophagy. Inflammation 43: 785-795, 2020.
49. Han X, Liu X, Zhao X, Wang X, Sun Y, Qu C, Liang J and Yang B: Dapagliflozin ameliorates sepsis-induced heart injury by inhibiting cardiomyocyte apoptosis and electrical remodeling through the PI3K/Akt pathway. Eur J Pharmacol 955: 175930, 2023.
50. Salvador JM, Brown-Clay JD and Fornace AJ Jr: Gadd45 in stress signaling, cell cycle control, and apoptosis. Adv Exp Med Biol 793: 1-19, 2013.
51. Xu W, Jiang T, Shen K, Zhao D, Zhang M, Zhu W, Liu Y and Xu C: GADD45B regulates the carcinogenesis process of chronic atrophic gastritis and the metabolic pathways of gastric cancer. Front Endocrinol (Lausanne) 14: 1224832, 2023.
52. Xie M, Xie R, Huang P, Yap DYH and Wu P: GADD45A and GADD45B as novel biomarkers associated with chromatin regulators in renal Ischemia-reperfusion injury. Int J Mol Sci 24: 11304, 2003.
53. Kim MY, Seo EJ, Lee DH, Kim EJ, Kim HS, Cho HY, Chung EY, Lee SH, Baik EJ, Moon CH and Jung YS: Gadd45beta is a novel mediator of cardiomyocyte apoptosis induced by ischaemia/hypoxia. Cardiovasc Res 87: 119-126, 2010.
54. Sheng M, Huang Z, Pan L, Yu M, Yi C, Teng L, He L, Gu C, Xu C and Li J: SOCS2 exacerbates myocardial injury induced by ischemia/reperfusion in diabetic mice and H9c2 cells through inhibiting the JAK-STAT-IGF-1 pathway. Life Sci 188: 101-109, 2017.
55. Tigno-Aranjuez JT, Asara JM and Abbott DW: Inhibition of RIP2's tyrosine kinase activity limits NOD2-driven cytokine responses. Genes Dev 24: 2666-2677, 2010.
56. Tian E, Zhou C, Quan S, Su C, Zhang G, Yu Q, Li J and Zhang J: RIPK2 inhibitors for disease therapy: Current status and perspectives. Eur J Med Chem 259: 115683, 2023.
57. Zhao W, Leng RX and Ye DQ: RIPK2 as a promising druggable target for autoimmune diseases. Int Immunopharmacol 118: 110128, 2023.
58. Pham AT, Ghilardi AF and Sun L: Recent advances in the development of RIPK2 modulators for the treatment of inflammatory diseases. Front Pharmacol 14: 1127722, 2023.
59. You J, Wang Y, Chen H and Jin F: RIPK2: A promising target for cancer treatment. Front Pharmacol 14: 1192970, 2023.
60. Zhao CH, Ma X, Guo HY, Li P and Liu HY: RIP2 deficiency attenuates cardiac hypertrophy, inflammation and fibrosis in pressure overload induced mice. Biochem Biophys Res Commun 493: 1151-1158, 2017.
61. Andersson L, Scharin Täng M, Lundqvist A, Lindbom M, Mardani I, Fogelstrand P, Shahrouki P, Redfors B, Omerovic E, Levin M, *et al*: Rip2 modifies VEGF-induced signalling and vascular permeability in myocardial ischaemia. Cardiovasc Res 107: 478-486, 2015.
62. Zhang J, Wang M, Ye J, Liu J, Xu Y, Wang Z, Ye D, Zhao M and Wan J: The Anti-inflammatory mediator resolvin E1 protects mice against Lipopolysaccharide-Induced heart injury. Front Pharmacol 11: 203, 2020.
63. Brown KA, Brain SD, Pearson JD, Edgeworth JD, Lewis SM and Treacher DF: Neutrophils in development of multiple organ failure in sepsis. Lancet 368: 157-169, 2006.
64. Li J, Xiao F, Lin B, Huang Z, Wu M, Ma H, Dou R, Song X, Wang Z, Cai C, *et al*: Ferrostatin-1 improves acute sepsis-induced cardiomyopathy via inhibiting neutrophil infiltration through impaired chemokine axis. Front Cell Dev Biol 12: 1510232, 2024.
65. Zhou S, Xu Y, Tu J and Zhang M: Inhibiting NLRP3/Caspase-1/GSDMD-mediated pyroptosis: A new role of GADD45B's role in hypertriglyceridemia-induced acute pancreatitis. Discov Med 37: 1105-1116, 2025.

66. Goh FY, Cook KL, Upton N, Tao L, Lah LC, Leung BP and Wong WS: Receptor-interacting protein 2 gene silencing attenuates allergic airway inflammation. J of Immunol 191: 2691-2699, 2013.
67. Chen XS, Wang SH, Liu CY, Gao YL, Meng XL, Wei W, Shou ST, Liu YC and Chai YF: Losartan attenuates sepsis-induced cardiomyopathy by regulating macrophage polarization via TLR4-mediated NF-κB and MAPK signaling. Pharmacol Res 185: 106473, 2022.
68. Yang Y, Li XY, Li LC, Xiao J, Zhu YM, Tian Y, Sheng YM, Chen Y, Wang JG and Jin SW: γδ T/Interleukin-17A contributes to the effect of maresin conjugates in tissue regeneration 1 on Lipopolysaccharide-induced cardiac injury. Front Immunol 12: 674542, 2021.
69. Csiszar A and Ungvari Z: Synergistic effects of vascular IL-17 and TNFalpha may promote coronary artery disease. Med Hypotheses 63: 696-698, 2004.
70. Ahmad S, Ahmed MM, Hasan PMZ, Sharma A, Bilgrami AL, Manda K, Ishrat R and Syed MA: Identification and validation of Potential miRNAs, as biomarkers for sepsis and associated lung injury: A Network-based approach. Genes (Basel) 11: 1327, 2020.
71. Wu K, Hu M, Chen Z, Xiang F, Chen G, Yan W, Peng Q and Chen X: Asiatic acid enhances survival of human AC16 cardiomyocytes under hypoxia by upregulating miR-1290. IUBMB Life 69: 660-667, 2017.
72. Tigno-Aranjuez JT, Benderitter P, Rombouts F, Deroose F, Bai X, Mattioli B, Cominelli F, Pizarro TT, Hoflack J and Abbott DW: In vivo inhibition of RIPK2 kinase alleviates inflammatory disease. J Biol Chem 289: 29651-2964, 2014.